Journal of Thermal Science Vol.27, No.3 (2018) 230–240

https://doi.org/10.1007/s11630-018-1004-5 **Article ID:1003-2169(2018)03-0230-11**

Thermodynamic Analysis of a Mixed Refrigerant Ejector Refrigeration Cycle Operating with Two Vapor-liquid Separators

TAN Yingying[1,2], CHEN Youming[1*], WANG Lin[2*]

1. School of Civil Engineering, Hunan University, Changsha, 410082, China
2. Institute of Refrigeration and Air-Conditioning, Henan University of Science and Technology, Luoyang, 471023, China

Abstract: A mixed refrigerant ejector refrigeration cycle operating with two-stage vapor-liquid separators (MRERC2) is proposed to obtain refrigeration temperature at -40°C. The thermodynamic investigations on performance of MRERC2 using zeotropic mixture refrigerant R23/R134a are performed, and the comparisons of cycle performance between MRERC2 and MRERC1 (MRERC with one-stage vapor-liquid separator) are conducted. The results show that MRERC2 can achieve refrigeration temperature varying between -23.9°C and -42.0°C when ejector pressure ratio ranges from 1.6 to 2.3 at the generation temperature of 57.3-84.9°C. The parametric analysis indicates that increasing condensing temperature decreases coefficient of performance (*COP*) of MRERC2, and increasing ejector pressure ratio and mass fraction of the low boiling point component in the mixed refrigerant can improve *COP* of MRERC2. The MRERC2 shows its potential in utilizing low grade thermal energy as driving power to obtain low refrigeration temperature for the ejector refrigeration cycle.

Keywords: Ejector Refrigeration; Zeotropic Refrigerant; Vapor-liquid Separator; Refrigeration Temperature

1. Introduction

Ejector refrigeration cycle (ERC) has gained increasing attention for energy-saving and environment-friendly purposes due to its potential of utilizing low grade thermal energy sources over a span of temperatures from 50°C to 100°C, such as solar energy, geothermal energy and industrial waste heat. However, the primary disadvantage of conventional ERC is that its *COP* is relatively low compared to other types of refrigeration cycles, which has greatly limited its widespread application. Therefore, in order to promote the application of ERC, much research work has been carried out to improve its performance, mainly focusing on refrigerant selection, ejector modeling and cycle optimization. Firstly, the performance of ERC is dependent on thermodynamic properties of the working fluid [1]. Considerable efforts have been concentrated on the performance of ERC using various refrigerants. Sun [2] compared the performance of ERC using eleven refrigerants and found that the cycle using R152a as refrigerant had better performance. Selvaraju et al. [3] compared the ejector performance using the environmentally friendly working fluids R290, R134a, R152a, R600a and R717. They found that R134a had a better performance in comparison with other refrigerants. Alexis et al. [4] simulated the performance of an ejector

Received: February 15, 2018 Corresponding author: CHEN Youming, Professor, E-mail: ymchen@hnu.edu.cn;
WANG Lin, Professor, E-mail: wlhaust@163.com
This study is financially supported by the National Natural Science Foundation of China (NSFC) (Grant No. 51706061&50706060)

Nomenclature

COP	coefficient of performance	*d*	diffuser
f_1	the ratio of the mass flow rate of the refrigerant flowing through the throttling valve 1 to that of the refrigerant coming from the bottom of the vapor-liquid separator 1	*e*	evaporator
f_m	the main stream ratio, i.e. the ratio of the mass flow rate of the refrigerant passing through the evaporator to that of the refrigerant passing through the condenser	*eo*	outlet of evaporator
h	enthalpy, kJ/kg	*g*	generator
m	mass flow rate, kg/s	*m*	mixing section
p	pressure, MPa	*mf*	mixed flow
PR	the pressure ratio of ejector	*min*	the minimum value
Q	heat or cooling capacity, kW	*n*	nozzle
t	temperature, °C	*n*1	inlet of the nozzle
Δt	temperature difference, °C	*n*2	outlet of the nozzle
u	velocity, m/s	*p*	circulation pump
W	power consumption of pump, kW	*pf*	primary flow
z	mass fraction of the volatile (low boiling point) component of the mixed refrigerant	*r*1	recuperator 1
Greek symbols		*r*2	recuperator 2
η	isentropic efficiency	*s*	isentropic process
μ	entrainment ratio of the ejector	1, 2, …,14	numbers for the states
Subscripts		1b	number for the state of the primary flow at the isentropic expansion at the nozzle exit of the ejector
c	condenser	2m	number for the state of the mixed flow at the constant pressure mixing in the mixing section of the ejector

cooling system driven by solar energy using R134a as working fluid and found that the *COP* of ejector refrigeration cycle varied from 0.035 to 0.199 with the evaporator temperature increasing from -10 to 0°C. Roman et al. [5] investigated the theoretical behavior of an ejector cooling system, using working fluids propane, butane, isobutane, R152a and R134a. The results showed that the system using propane had the highest *COP*. Chen et al. [6] selected various refrigerants (R134a, R152a, R290, R430a, R245fa, R600, R600a, R1234ze and R436B) and compared their performances and applicabilities in an ejector refrigeration system. The comparison results indicated that R600 was a good candidate for the ejector refrigeration system due to a relatively high *COP* and its low environmental impact. These studies all indicate that the appropriate working fluid can yield good performance for ERC under the selected operating conditions. Secondly, since the ejector performance is critical to the performance, capability, size and cost of the whole ERC, constructing valid mathematical models of the ejector has become the key subject of many studies [7,8]. Huang et al. [9] carried out a 1-D analysis for the prediction of ejector performance at critical-mode operation and reported that the 1-D analysis using the empirical coefficients could accurately predict the performance of the ejectors. Ouzzane and Aidoun [10] developed the model and computer programs of ejectors for the optimal ejector design and detailed simulation of ERC. Cizungu et al. [11] established a one-dimensional compressible flow model to simulate and optimize one and two-phase ejectors under steady-state operation condition based on the control volume approach. Zhu and Li [12] proposed a novel ejector model for the performance evaluation on ejectors at critical operating mode and found that the model had a good performance in predicting the mass flow rate and the entrainment ratio for ejectors. In order to take account of both ideal and real gases, Cardemil and Colle [13] developed an ejector model for the evaluation of vapor ejector performance and found that the proposed model provided reliable estimations in terms of ejector performance (entrainment ratio and critical back-pressure). Chen et al. [14] proposed a new model to predict ejector

performance over both critical and sub-critical operation modes. All these mathematical models have been constructed to analyze and predict ejector performance as well as optimize design parameters. Thirdly, the performance enhancement of ERC is possibly attained through cycle optimization, and many advanced cycles have been proposed. Zhang and Shen [15] proposed a new bi-ejector refrigeration cycle, in which a vapor-liquid ejector replaced the mechanical pump to convey the condensate back to the generator. Thus, no electricity consumption was required. Yu et al. [16] proposed a novel ejector refrigeration cycle, in which an additional jet pump was used in ERC to decrease the ejector pressure ratio for the improvement of cycle performance. Sokolov and Hershgal [17] proposed the booster assisted ejector cycle. In this cycle, the low-pressure ratio mechanical-driven compressor was placed between the evaporator outlet and ejector suction line to increase the ejector suction pressure, causing an increase of the cycle performance. Sun [18] studied a combined ejector-vapor compression cycle and the results showed that the combined cycle could improve *COP* by more than 50% over the conventional cycles. Chesi et al. [19] also analyzed a complex system in which the solar powered ejection machine was used to increase the efficiency of a traditional vapor compression machine by subtracting heat from the condenser and evaluated the potential advantages of the hybrid system. Obviously, these advanced cycles either introduced an additional ejector into the conventional ERC, or adopted a combination of thermal and mechanical energy to enhance the performance of ERC. Although these advanced cycles can greatly enhance the performance of ERC, the additional components make the proposed cycles more complicated in practical applications and the enhancement of performance is attained at the cost of additional mechanical energy consumption for the hybrid compressor and ejector refrigeration cycles.

Previous researches have demonstrated that the appropriate choice of refrigerants, the valid mathematical model of ejector and the improved cycle configuration can significantly improve the performance of ERC. However, the conventional ERC using pure substance as refrigerant cannot obtain low refrigeration temperature, and its refrigeration temperature is always above -10°C in practical applications. The reason is that high pressure ratio risk appears for the ejector with refrigeration temperature reduction and the corresponding entrainment ratio of ejector and *COP* of conventional ERC decrease dramatically. Therefore, there are few studies on the ERC for low refrigeration temperature application. However, in many production processes, such as food industry, pharmaceutical industry and chemical engineering, there is not only a lot of available waste heat but also a great deal of cooling and freezing demands in low temperatures [20], so it is of practical significance to develop a novel ERC for low temperature applications.

As is known, zeotropic mixture refrigerant with composition shift at vapor-liquid equilibrium state can be used to obtain a lower refrigeration temperature with a moderate pressure ratio in simple mechanical compression refrigeration cycle [22-25]. Therefore, if the thermodynamic property of zeotropic mixture is employed in heat-driven ERC, it perhaps contributes to obtaining lower refrigeration temperature in ERC. Based on the principle, a mixed refrigerant ERC operating with one vapor-liquid separator (MRERC1) is proposed and the cycle performance is investigated theoretically [26]. The results indicate that the MRERC1 can achieve the refrigeration temperature of -30°C, while the ejector pressure ratio is at least 3.0. However, it is still difficult for the ejector to operate under the working condition of such high pressure ratio in practical applications. Therefore, a mixed refrigerant ERC operating with two vapor-liquid separators (MRERC2) is proposed in this paper. The thermodynamic performance characteristics of MRERC2 are investigated theoretically.

2. Cycle description

In order to obtain lower refrigeration temperature in heat-driven ERC, MRERC2 is proposed as shown in Fig. 1(a). The corresponding cycle pressure enthalpy diagram is demonstrated in Fig. 1(b). The proposed MRERC2 consists of an ejector, a generator, a condenser, an evaporator, a circulation pump, two recuperators, two vapor-liquid separators and three throttling valves. The principle of multi-stage separation, condensation and purification of vapor-liquid two-phase mixtures with descending boiling point component is applied to the MRERC2. In this cycle, the vapor-liquid separator divides a high pressure zeotropic mixture into two fractions: a liquid fraction enriched with the high-boiling component and a vapor fraction enriched with the low-boiling component. The liquid fraction passes through a throttling valve to provide refrigeration for precooling the separated vapor fraction. The vapor fraction then goes down to provide refrigeration at lower temperature level [27]. This character of zeotropic mixture refrigerant offers the possibility to obtain low refrigeration temperature with a heat-driven ejector that can only provide relatively low pressure ratio.

The mixture R23/R134a is widely used zeotropic mixture refrigerant. The normal boiling point of R134a is -26.07°C, and the normal boiling point of R23 is -82.06°C. The boiling points and boiling point gaps of R134a and R23 (55.99°C) both are satisfactory for high boiling component and low boiling component separation [27, 28]. Thus, the zeotropic mixture R23/R134a is used

as the refrigerant of MRERC2 in this paper, and R23 is the low boiling component of the mixed refrigerant.

The main working principle of MRERC2 using zeotropic mixture R23/R134a is described as follows: The R134a-rich vapor coming from the generator firstly enters the nozzle of ejector as primary flow to entrain the secondary flow from the low pressure passage of the recuperator 1, then it mixes with the secondary flow in the mixing section of ejector and recovers a pressure lift in the diffuser of the ejector. The refrigerant mixture vapor discharged from the ejector goes through the condenser and is partially condensed. Then it flows into the vapor–liquid separator 1 where the vapor and liquid phases of the mixed refrigerant are separated. The vapor, which is rich in R23, flows from the top of vapor–liquid separator 1, while the liquid rich in R134a flows out of the bottom of vapor–liquid separator 1. The vapor refrigerant then flows into the high pressure passage of recuperator 1 and partially condenses. As the vapor-liquid mixture from the recuperator 1 enters the vapor-liquid separator 2, it undergoes phase separation as well in the vapor-liquid separator 2. After the R23-rich vapor from the top of the vapor-liquid separator 2 flows through the high pressure passage of recuperator 2 and condenses, it passes through the throttling valve 3, throttling and expanding to the vapor-liquid refrigerant of lower temperature. It then enters the evaporator and vaporizes to realize the refrigeration effect, leaving as the saturated vapor. The R134a-rich liquid out of the bottom of the vapor–liquid separator 2 enters the throttling valve 2, expanding into the low temperature state, and then mixes with the lower temperature vapor from the evaporator. This low temperature vapor-liquid mixture flows into the low pressure passage of recuperator 2 to condense the vapor from the top of the vapor-liquid separator 2. The R134a-rich saturated liquid from the bottom of the vapor–liquid separator1 is separated into two streams. One stream passes through the throttling valve 1, expanding to the low-temperature refrigerant. Then it mixes with the refrigerant from the low pressure passage of recuperator 2, and the mixed refrigerant flows into the low pressure passage of the recuperator 1 to condense the vapor refrigerant from the top of vapor-liquid separator 1, leaving as slightly superheated vapor and entering the ejector as secondary flow. The other stream returns back to the circulation pump and then enters the generator, leaving as the saturated or superheated vapor. Then it enters the ejector as the primary flow. The cycle is completed.

The schematic diagram of MRERC1 is shown in Fig.2. The difference between MRERC1 and MRERC2 is that MRERC2 operates with two vapor-liquid separators, while MRERC1 operates with one vapor-liquid separator. The introduced two vapor-liquid separators in MRERC2 have the advantage of increasing the mass fraction of the low boiling component in zeotropic refrigerant mixture that enters the evaporator, lowering the ejector pressure ratio at the same refrigeration temperature. Thus, the proposed MRERC2 helps obtain lower refrigeration temperature and provide low pressure ratio operating condition for the ejector, which can greatly boost the practical application potential of MRERC.

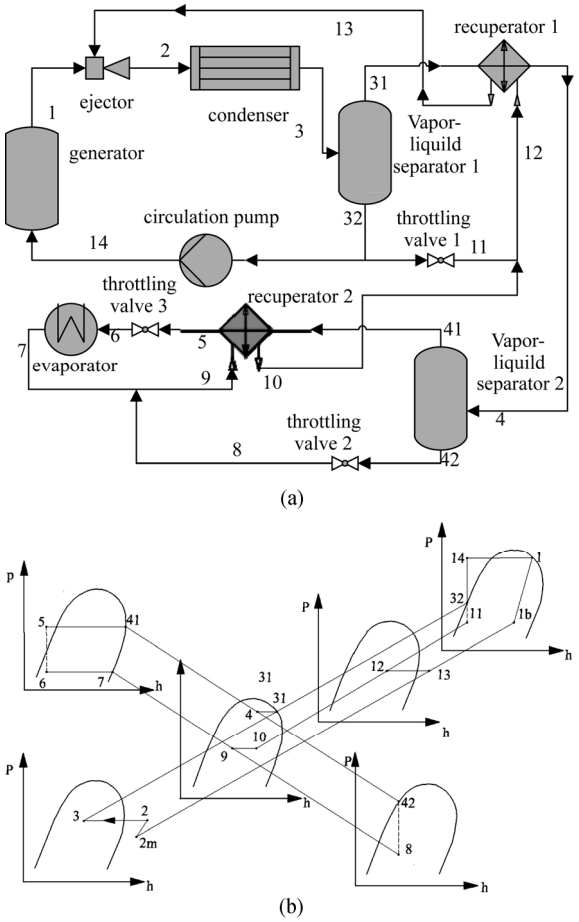

Fig. 1 Schematic diagrams (a) and pressure-enthalpy diagram (b) of mixed refrigerant ERC operating with two vapor–liquid separators.

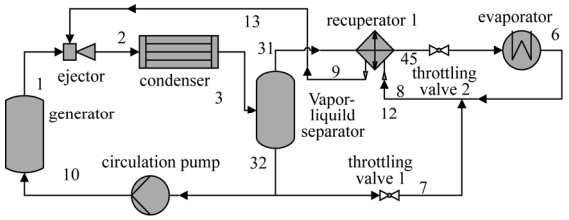

Fig. 2 Schematic diagram of mixed refrigerant ERC operating with one vapor-liquid separator

3. Mathematical model

3.1 Ejector model

Ejector is the key component in the novel cycle, and

COP of the cycle depends strongly on the performance of the ejector. In the present study, the ejector performance simulation is carried out based on the one-dimensional constant pressure flow model [9, 29, 30].

To simulate the ejector, the following assumptions are made.

1. The flow inside the ejector is in steady state and one-dimensional.

2. Velocities of streams at the inlet and outlet of the ejector could be negligible.

3. The effects of frictional and mixing losses in the nozzle, mixing section and diffuser of ejector are taken into account by using the nozzle efficiency η_n, the mixing efficiency η_m, and the diffuser efficiency η_d.

4. Mixing process in the mixing section of the ejector occurs at constant pressure and complies with the conservation of energy and momentum.

5. The flow process in the ejector is assumed adiabatic.

Based on mass, energy and momentum conservation can be derived as

$$\mu = \sqrt{\eta_n \eta_m \eta_d (h_{pf,n1} - h_{pf,n2,s})/(h_{mf,d,s} - h_{mf,m})} - 1 \quad (1)$$

Where $h_{pf,n1}$ is inlet enthalpy of primary flow, $h_{pf,n2,s}$ is the ideal exit enthalpy of the primary flow under the isentropic expansion, $h_{mf,d,s}$ is the ideal exit enthalpy of the mixed flow under the isentropic compression, $h_{mf,m}$ is the enthalpy of mixed flow and η_n is the nozzle efficiency, η_d is the diffuser efficiency, η_m is the mixing efficiency.

3.2 Cycle model

The mathematical models are developed to analyze the performance of the novel cycle. For the cycle simulation, the following assumptions are also made.

1. The cycle reaches a steady state, and heat loss to the environment is neglected.

2. The flow across the throttling valves is isenthalpic.

3. The evaporator outlet state is saturated vapor.

4. The vapor streams from the top of the vapor-liquid separators are saturated vapor and the liquid streams from the bottom of vapor-liquid separator are saturated liquid. The vapor stream coming from the generator is saturated vapor.

5. The minimum temperature differences in the recuperators 1 and 2 are specified as $\Delta t_{r1.min}$ and $\Delta t_{r2.min}$ which occur at the hot end of recuperator 1 and the cold end of recuperator 2, respectively.

6. The pressure losses in the cycle are neglected except in the throttling valves.

For the energy analysis of the novel cycle, the basic models for all the components are set up by applying the principles of mass conservation and energy conservation. The basic equations of each component are given respectively as follows.

For evaporator:

$$Q_e = m_5(h_7 - h_6) \quad (2)$$

For generator:

$$Q_g = m_1(h_1 - h_{14}) \quad (3)$$

For condenser:

$$Q_c = m_2(h_2 - h_3) \quad (4)$$

For recuperator 1:

$$Q_{r1} = m_4(h_{31} - h_4) = m_{12}(h_{13} - h_{12}) \quad (5)$$

For recuperator 2:

$$Q_{r2} = m_5(h_{41} - h_5) = m_9(h_{10} - h_9) \quad (6)$$

For the circulation pump:

$$W = m_1(h_{14,s} - h_{32})/\eta_p \quad (7)$$

Where, η_p is the pump efficiency.

The mixed refrigerant from the condenser undergoes twice phase separations in the vapor-liquid separator 1 and 2. Hence:

$$f_m = x_3 \cdot x_4 = m_5 / m_2 \quad (8)$$

Where, f_m is the main stream ratio, i.e. the ratio of the mass flow rate of the refrigerant passing through the evaporator to that of the refrigerant passing through the condenser, x_3 and x_4 are the quality of mixed refrigerant at states 3 and 4.

The *COP* of the cycle can be defined as the ratio of the cooling capacity to the sum of the heat input of the generator and the power input of the circulation pump. It is written as follows:

$$COP = Q_e/(Q_g + W) \quad (9)$$

The ejector entrainment ratio is defined as the ratio of the ejector secondary mass flow rate (state 13) to the primary mass flow rate (state 1). Therefore,

$$\mu' = \frac{m_{13}}{m_1} = \frac{x_3 + (1 - x_3) \cdot f_1}{(1 - x_3) \cdot (1 - f_1)} \quad (10)$$

Where f_1 is the ratio of the mass flow rate of the refrigerant passing through the throttling valve 1 to that of the refrigerant coming from the bottom of the vapor-liquid separator 1.

Using the equations described above, calculations can be carried out to determine the entrainment ratio, generating temperature and *COP* of the new cycle under the given operating conditions. It should be noted that in the simulation procedure, the entrainment ratio of the ejector must satisfy a mass balance for steady-state operation of the cycle, i.e., at the same time, under the given operating conditions, the entrainment ratio of the ejector can be determined by the primary flow and secondary flow as well as the ejector outlet pressure [31]. In this case, under the condition that the secondary flow and ejector outlet pressure are known, by adjusting the generation temperature, the solution converges to the ejector entrainment ratio (μ) required by the steady-state operation of the cycle. The procedure of the numerical computation is

shown in Fig. 3. Based on the flowchart for the simulation, the calculation program is written with FORTRAN language. And thermodynamic properties of refrigerant mixture are calculated based on data from the NIST REFPROP database [32]. In the next section, the performance characteristic of the cycle and the effects of some parameters on the cycle performance are investigated.

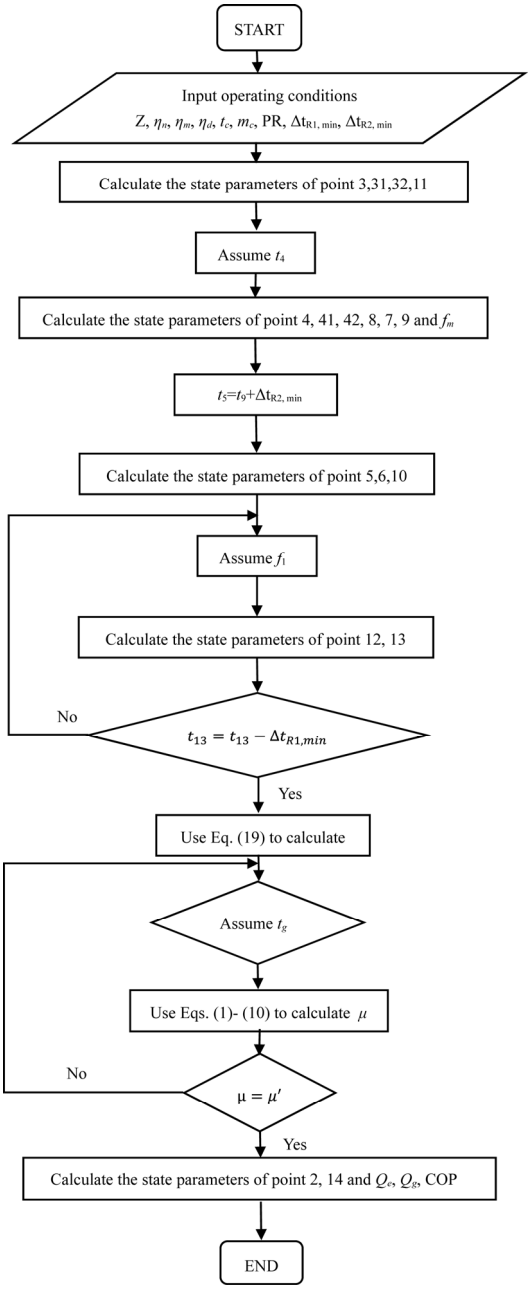

Fig. 3 Flow chart for the calculation of MRERC2

4. Results and discussion

4.1 Effects of ejector pressure ratio

To evaluate the effects of ejector pressure ratio on MRERC2, the performance of MRERC2 is simulated under the following operation condition, the ejector pressure ratio (*PR*) ranging from 1.6 to 2.3, the initial charge mass fraction of R23 z_3 = 0.20, the condenser outlet temperature t_c = 20°C, the condensation pressure p_c = 1.2 MPa and the mass flow rate of refrigerant through the condenser is 1 kg·s^{-1}.

Fig. 4 shows the variation of evaporation pressure (p_e) and evaporator inlet temperature (t_e) with the ejector pressure ratio (*PR*). It can be seen that the evaporation pressure and evaporator inlet temperature decrease as the ejector pressure ratio increases. The reason is that the evaporation pressure decreases when the ejector pressure ratio increases at the constant condensation pressure, resulting in a decreasing evaporator inlet temperature. It should be noted that the evaporator inlet temperature ranges from -23.9°C to -42.0°C at the ejector pressure ratio varying from 1.6 to 2.3 under the given operating conditions. When the ejector pressure ratio is 2.3, the evaporator inlet temperature can reach -42.0°C. Through theoretical calculation, Alexis et al. [4, 33] obtained a refrigerating temperature of -10°C in conventional ERC using R134a and methanol as its refrigerant, which was the lowest refrigeration temperature obtained by the ERC in earlier work. It is obvious that the lowest refrigerating temperature obtained by the proposed MRERC2 is much lower than that obtained by the conventional ERC in the literatures up to now.

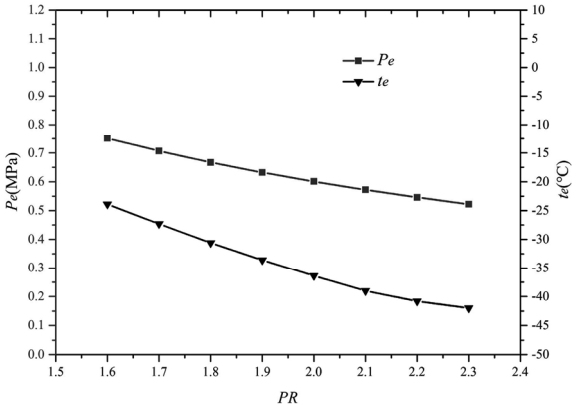

Fig. 4 Variation of p_e and t_e with *PR*

Fig.5 shows the variation of the ratio of the mass flow rate of the refrigerant passing through the throttling valve 1 to that of the refrigerant coming from the bottom of the vapor-liquid separator 1 (f_1) the ejector entrainment ratio (μ) and the generation temperature (t_g) with the ejector pressure ratio (*PR*). It could be observed that the ejector entrainment ratio and generation temperature increase as the ejector pressure ratio increasing. The reason is that the heat exchange capacity of recuperator 2 can be increased by a decrease of the evaporator outlet temperature and then the refrigerant mass flow rate through the throttling valve 1 increases to ensure the minimum tem-

perature differences at the hot end of the recuperators 1, resulting in an increase of f_1. Thus, according to Eq. (10), the ejector entrainment ratio will increase to maintain the stable operating condition of the new cycle. The increase of both entrainment ratio and the ejector pressure ratio cause an increase of generation temperature. Under the given conditions, the ejector entrainment ratio and generation temperature range from 0.162 to 0.188 and from 57.3°C to 84.9°C at the ejector pressure ratio varying from 1.6 to 2.3, respectively.

Fig. 6 shows the variation of the refrigeration capacity (Q_e), the heating capacity of generator (Q_g) and the *COP* of the proposed cycle with the ejector pressure ratio (*PR*). It could be found that the refrigeration capacity increases as the ejector pressure ratio increasing. As the ejector pressure ratio rises, the refrigeration capacity per unit mass flow rate increases for the increasing inlet subcooling of throttling valve 3. With the fixed refrigerant mass flow rate through the evaporator, the refrigeration capacity increases. It could also be observed that the heating capacity of generator decreases with the increasing ejector pressure ratio. On the one hand, the heating capacity per unit mass flow rate decreases as generation temperature increases. On the other hand, the refrigerant mass flow rate through the generator decreases with the increase of the refrigerant mass flow rate through the

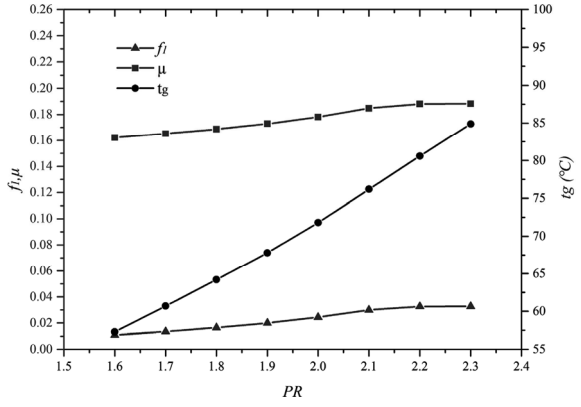

Fig. 5 Variation of f_1, μ and t_g with PR

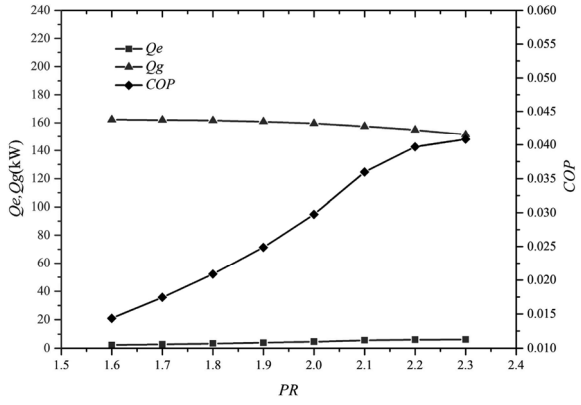

Fig. 6 Variation of Q_e, Q_g and *COP* with *PR*

throttling valve 1. The decrease of mass flow rate and the decrease of heating capacity of unit mass flow rate together make the heating capacity of generator decrease. It is concluded that the *COP* of the new cycle increases with the increasing ejector pressure ratio. Under the given conditions, the *COP* of new cycle ranges from 0.014 to 0.041 at the ejector pressure ratio varying from 1.6 to 2.3.

4.2 Effects of condenser outlet temperature

To evaluate the effects of condenser outlet temperature on MRERC2, the performance of MRERC2 is simulated under the following operation condition, condenser outlet temperature (t_c) ranging from 18°C to 24°C, the pressure ratio of ejector is 2.3, the refrigerant steam quality at the condenser outlet is 0.13, the initial charge mass fraction of R23 and the mass flow rate of refrigerant through the condenser is 1 kg·s^{-1}.

Fig. 7 shows the variation of the mass fraction of R23 at point 41 (z_{41}), evaporation pressure (p_e) and evaporator inlet temperature (t_e) with condenser outlet temperature (t_c) under the given condition. It could be observed that the mass fraction of R23 at state 41, the evaporation pressure and evaporator inlet temperature increase as increasing condenser outlet temperature. For the fixed refrigerant steam quality at the condenser outlet, the condensation pressure increases with increasing the condenser outlet temperature, resulting in the increasing evaporation pressure. Due to the increasing condensation pressure and constant temperature at state point 4, the mass fraction of R23 at state 41 increases. The evaporator inlet temperature is not only influenced by evaporation pressure but also the mass fraction of R23 at state 41, and the former is more important in this case. Thus, the evaporator inlet temperature increases. Under the given conditions, the evaporation pressure and evaporator inlet temperature range from 0.496 MPa to 0.578 MPa and from -42.7°C to -40.4°C as the condenser outlet temperature varies from 18°C to 24°C.

Fig. 8 shows the variation of the ratio of the mass flow rate of the refrigerant passing through the throttling valve 1 to that of the refrigerant coming from the bottom of the vapor-liquid separator 1 (f_1), the ejector entrainment ratio (μ) and the generation temperature (t_g) with condenser outlet temperature (t_c). It could be seen that the ejector entrainment ratio and generation temperature both decrease with increasing condenser outlet temperature. The reason is that as the condenser outlet temperature increases, the condensation pressure increases, resulting in a decreasing refrigerant quality of state 4. Thus, the main stream ratio (f_m) decreases. The heat exchange capacity of recuperator 2 drops with a decreasing main stream ratio and then the refrigerant mass flow rate through the

throttling valve 1 decreases to ensure the minimum temperature differences at the hot end of the recuperators 1, resulting in a decrease of f_1. Thus, according to Eq. (10), the ejector entrainment ratio will decrease to maintain the stable operation of the new cycle. For the fixed ejector pressure ratio, the decrease of ejector entrainment ratio causes a decrease of generation temperature. Under the given operating conditions, the ejector entrainment ratio and generation temperature range from 0.204 to 0.153 and from 85.5°C to 82.7°C at the condenser outlet temperature varying from 18°C to 24°C, respectively.

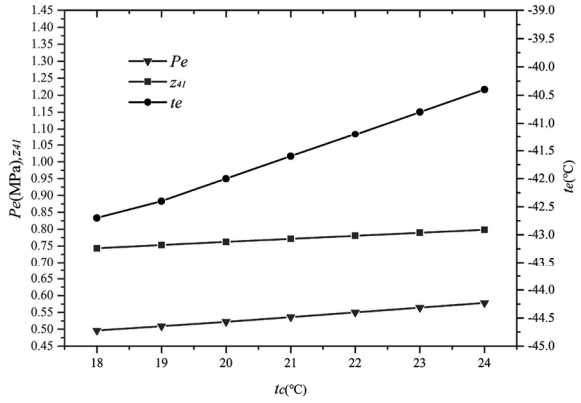

Fig. 7 Variation of p_e, z_{41} and t_e with t_c

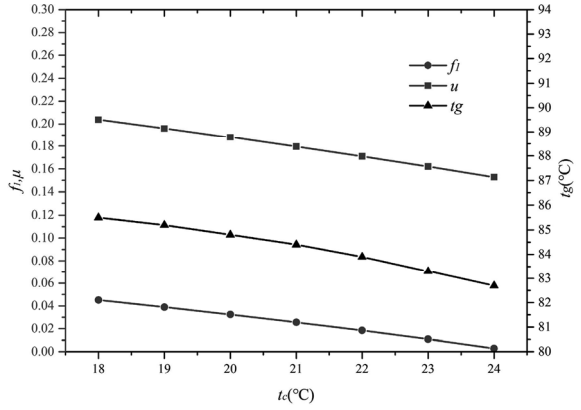

Fig. 8 Variation of f_1, μ and t_g with t_c

Fig. 9 shows the variation of the refrigeration capacity (Q_e), the heating capacity of generator (Q_g) and the *COP* of the cycle with condenser outlet temperature (t_c). It is shown that the refrigeration capacity decreases and the heating capacity of generator increases as the condenser outlet temperature increases. The refrigeration capacity decreases for the decreasing mass flow rate through the evaporator, and the heating capacity of generator increases because of the increasing mass flow rate through the generator. Due to the combined effects of the refrigeration capacity and heating capacity of generator, the *COP* of the new cycle decreases with increasing condenser outlet temperature. Under the given conditions, the *COP* of new cycle ranges from 0.054 to 0.011 as the condenser outlet temperature varies from 18°C to 24°C. Thus, the results show that the decrease of condenser outlet temperature can significantly improve the cycle performance.

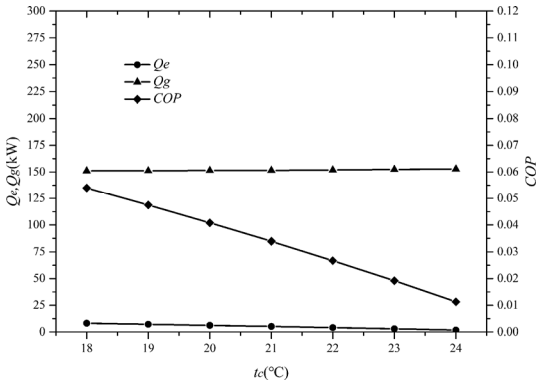

Fig. 9 Variation of Q_e, Q_g and *COP* with t_c

4.3 Effects of refrigerant mixture composition

To evaluate the effects of refrigerant mixture composition on MRERC2, the performance of MRERC2 is simulated under the following operation condition, the initial charge mass fraction of R23 (z_3) ranging from 0.10 to 0.22, the pressure ratio of ejector is 2.2, the refrigerant steam quality at the condenser outlet is 0.13, the condenser outlet temperature t_c is 20°C and the mass flow rate of refrigerant through condenser is 1 kg·s^{-1}.

Fig. 10 shows the variation of evaporation pressure (p_e), the mass fraction of R23 at state 41 (z_{41}) and evaporator inlet temperature (t_e) with the initial charge mass fraction of R23 (z_3). It is shown that the evaporation pressure and the mass fraction of R23 at state 41 both increase as the initial charge mass fraction of R23 increases. The reason is that as the initial charge mass fraction of R23 increases, the condensation pressure increases, resulting in an increasing evaporation pressure. For the fixed temperature of state 4, the increase of condensation pressure causes an increase of mass fraction of R23 at state 41. It can also be seen that the evaporator inlet temperature fluctuates with the increase of initial charge mass fraction of R23. As the evaporation pressure increases, the evaporator inlet temperature increases. On the other hand, as the mass fraction of R23 at state 41 increases, the evaporator inlet temperature decreases. Thus, the increase of evaporation pressure and the increase of mass fraction of R23 at state 41 have the opposite effect on the evaporator inlet temperature, resulting in the evaporator inlet temperature fluctuation. Under the given conditions, the evaporator inlet temperature ranges between -38°C to -40.8°C at the initial charge mass fraction of R23 varying from 0.10 to 0.22.

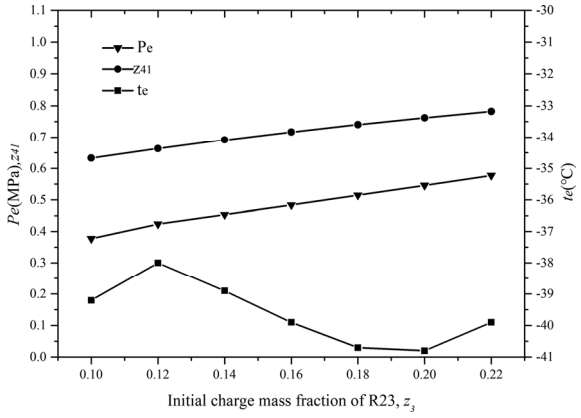

Fig. 10 Variation of p_e, z_{41} and t_e with z_3

Fig. 11 shows the variation of the ratio of the mass flow rate of the refrigerant passing through the throttling valve 1 to that of the refrigerant coming from the bottom of the vapor-liquid separator 1 (f_1), the ejector entrainment ratio (μ) and the generation temperature (t_g) with the initial charge mass fraction of R23 (z_3). It could be seen that the ejector entrainment ratio and generation temperature both increase with the increasing initial charge mass fraction of R23.The condensation pressure increases with increasing the initial charge mass fraction of R23, resulting in an increase of refrigerant quality at the inlet of vapor-liquid separator 2. Thus, the main stream ratio increases. The heat exchange capacity of recuperator 2 increases subsequently, which causes an increase of the refrigerant mass flow rate through the throttling valve 1, resulting in an increase of f_1. Thus, according to Eq. (10), the ejector entrainment ratio increases to ensure the stable operating condition of the new cycle. For the fixed ejector pressure ratio, the increase of ejector entrainment ratio causes an increase of generation temperature. Under the given conditions, the ejector entrainment ratio and generation temperature range from 0.159 to 0.188 and from 68°C to 82.3°C at the initial charge mass fraction of R23 varying from 0.10 to 0.22, respectively.

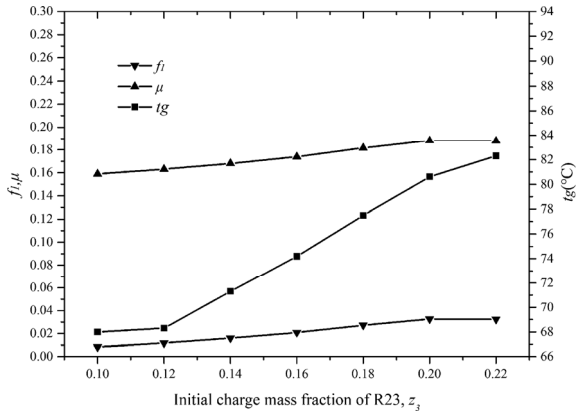

Fig. 11 Variation of f_1, μ and t_g with z_3

Fig. 12 shows the variation of the refrigeration capacity (Q_e), the heating capacity of generator (Q_g) and the *COP* of the cycle with initial charge mass fraction of R23 (z_3). It could be observed that the refrigeration capacity increases and the heating capacity of generator decreases as the initial charge mass fraction of R23 increases. The refrigeration capacity increases owing to the increasing mass flow rate through the evaporator, and the heating capacity of generator decreases because of the decreasing mass flow rate through the generator. Due to the combined effects of the refrigeration capacity and heating capacity of the generator, the *COP* of the new cycle increases with the increasing initial charge mass fraction of R23. Under the given conditions, the *COP* of new cycle ranges from 0.013 to 0.041 while the initial charge mass fraction of R23 varies from 0.10 to 0.22.

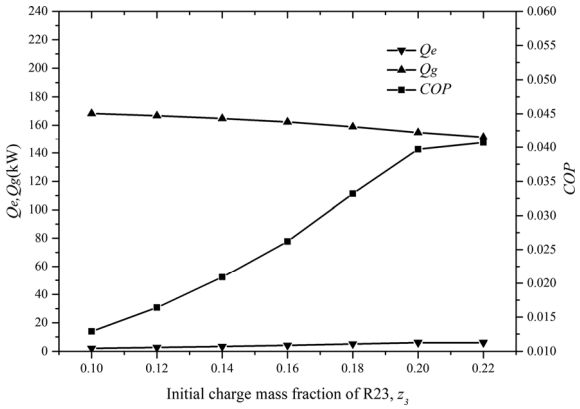

Fig. 12 Variation of Q_e, Q_g and *COP* with z_3

4.4 Comparison of MRERC and ERC

The cycle performance of the proposed MRERC2 is compared with that of conventional ERC and that of MRERC1 using mixed refrigerant R134a+R23 as their working fluids, and the key results are illustrated in Fig. 13 and Fig. 14.

In this calculation, the initial charge mass fraction of R23 (z_3) is 0.2, the condensation pressure is 1.2 MPa, the condenser outlet temperature is 20°C and the mass flow rate of refrigerant through condenser is 1 kg·s^{-1}. The evaporator outlet temperature t_{eo} is kept in a range of -22°C to -15°C.

Fig.13 shows the effect of the evaporator outlet temperature (t_{eo}) on the ejector pressure ratio (PR) of MRERC1, MRERC 2 and ERC. It can be found that as the evaporator outlet temperature increases, the ejector pressure ratios of the proposed MRERC 2, MCERC 1 and the conventional ERC decrease. The ejector pressure ratio in ERC varies in a range 8.29-6.15 and that in MRERC 1 varies in a range 4.63-3.45, which are unattainable for the ejector, while the ejector pressure ratio in MRERC 2 varies in a range 2.29-1.73, which is attainable for the ejector, when the evaporator outlet tempera-

ture ranges from -22°C to -15°C. It is shown that the ejector pressure ratios in ERC and MRERC1 are obviously much larger than that in MRERC 2, leading to high pressure ratio risk for ejector in ERC and MRERC1.

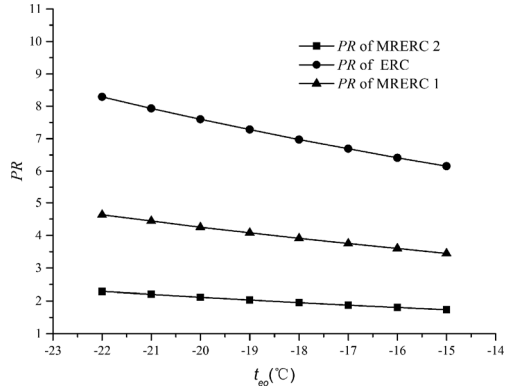

Fig. 13 Variation of PR with t_{eo}

Fig.14 shows the effect of the evaporator outlet temperature (t_{eo}) on the refrigeration capacity (Q_e) and *COP* of MRERC 1, MRERC 2 and ERC. It is observed that as the evaporator outlet temperature varies from -22°C to -15°C, the refrigeration capacity and *COP* of ERC and MRERC 1 are equal to zero. That is because the ejector cannot work at all under the condition of such high pressure ratios. That is, the conventional ERC and MRERC 1 cannot achieve such low refrigeration temperature under the same working condition. On the contrary, the refrigeration capacity of MRERC 2 varies from 6.18 kW to 2.99 kW, and *COP* of MRERC2 varies from 0.040 to 0.018, as the evaporator outlet temperature varies from -22°C to -15°C.

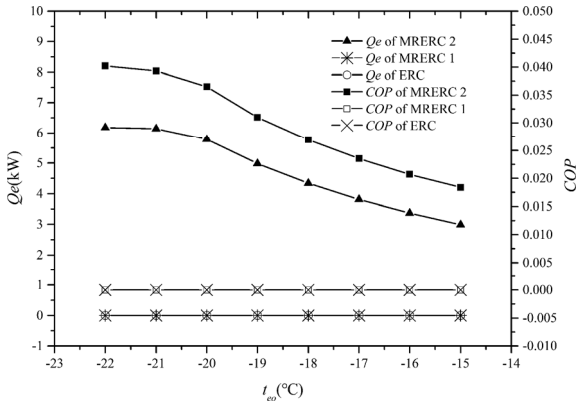

Fig. 14 Variation of Q_e and *COP* with t_{eo}

5. Conclusions

A mixed ejector refrigeration cycle operating with two vapor-liquid separators is proposed, which can achieve refrigeration temperature at -40°C temperature range under the low pressure ratio operating conditions of ejector. The performances of the proposed cycle are theoretically investigated based on the developed mathematical model, and then compared with that of the conventional ejector refrigeration cycle and that of the mixed refrigerant ejector refrigeration cycle operating with one vapor-liquid separator. The main conclusions of this study are summarized as follows:

The novel cycle can significantly decrease the refrigeration temperature without increasing the ejector pressure ratio. The cycle can achieve the lowest refrigeration temperature of -42.0°C when the pressure ratio of ejector is 2.3, the generation temperature is 84.9°C and the condenser outlet temperature is 20°C. Such low refrigeration temperature cannot be obtained by conventional ejector refrigeration cycle and mixed refrigerant ejector refrigeration cycle operating with one vapor-liquid separator under the same operating conditions.

Condenser outlet temperature, pressure ratio of the ejector and the refrigerant mixture composition have significant effects on the refrigeration temperature, the ejector entrainment ratio, generation temperature, refrigeration capacity, heating capacity of generator and *COP* of the proposed cycle.

The ejector pressure ratio in MRERC2 is obviously much lower than that in ERC and MRERC1, and it is feasible for MRERC2 to be applied to practical engineering projects because of lower pressure ratio for the ejector.

And it is also noted that additional studies, especially experimental studies are being carried out in our lab to verify the feasibility of the proposed cycle.

References

[1] Yu J. and Du Z.. Theoretical study of a transcritical ejector refrigeration cycle with refrigerant R143a. Renewable Energy, 2010, 35(9): 2034–2039.

[2] Sun D.W. Comparative study of the performance of an ejector refrigeration cycle operating with various refrigerants. Energy Conversion and Management, 1999, 40(8): 873–884.

[3] Selvaraju A. and Mani A. Analysis of a vapour ejector refrigeration system with environment friendly refrigerants. International Journal of Thermal Sciences, 2004, 43(9): 915–921.

[4] Alexis G. and Karayiannis E.. A solar ejector cooling system using refrigerant R134a in the Athens area. Renewable Energy, 2005, 30(9):1457–1469.

[5] Roman R. and HernandezJ.I.. Performance of ejector cooling systems using low ecological impact refrigerants. International Journal of Refrigeration, 2011, 34(7): 1707–1716.

[6] Chen J., Havtun H. and Palm B.. Screening of working

fluids for the ejector refrigeration system. International Journal of Refrigeration, 2014, 47: 1–14.

[7] He S., Li Y., and Wang R.Z.. Progress of mathematical modeling on ejectors. Renewable and Sustainable Energy Reviews, 2009, 13(8): 1760–1780.

[8] Besagni G, Mereu R, Inzoli F. CFD Study of Ejector Flow Behavior in a Blast Furnace Gas Galvanizing Plant. Journal of Thermal Science, 2015, 24(1): 58–66

[9] Huang B.J., et al. A 1-D analysis of ejector performance Analyse unidimensionnelle de la performance d'un éjecteur. International Journal of Refrigeration, 1999, 22(5): 354–364.

[10] Ouzzane M. and Aidoun Z.. Model development and numerical procedure for detailed ejector analysis and design. Applied Thermal Engineering, 2003, 23(18): 2337–2351.

[11] Cizungu K., Groll M., and Ling Z.G.. Modelling and optimization of two-phase ejectors for cooling systems. Applied Thermal Engineering, 2005, 25(13): 1979–1994.

[12] Zhu Y. and Li Y.. Novel ejector model for performance evaluation on both dry and wet vapors ejectors. International Journal of Refrigeration, 2009, 32(1): 21–31.

[13] Cardemil J. M. and Colle S.. A general model for evaluation of vapor ejectors performance for application in refrigeration. Energy Conversion and Management, 2012, 64: 79–86.

[14] Chen W., et al. A 1D model to predict ejector performance at critical and sub-critical operational regimes. International Journal of Refrigeration, 2013, 36(6): 1750–1761.

[15] Zhang B. and Shen S.. A theoretical study on a novel bi-ejector refrigeration cycle. Applied Thermal Engineering, 2006, 26(5–6): 622–626.

[16] Yu J., et al. A new ejector refrigeration system with an additional jet pump. Applied Thermal Engineering, 2006, 26(2-3): 312–319.

[17] Sokolov M. and Hershgal D.. Enhanced ejector refrigeration cycles powered by low grade heat. Part 1. Systems characterization. International Journal of Refrigeration, 1990, 13(6): 351–356.

[18] Sun D.W. Solar powered combined ejector-vapour compression cycle for air conditioning and refrigeration. Energy Conversion and Management, 1997, 38(5): 479–491.

[19] Chesi A., et al. Suitability of coupling a solar powered ejection cycle with a vapour compression refrigerating machine. Applied Energy, 2012, 97: 374–383.

[20] He Y. and Chen G.. Experimental study on an absorption refrigeration system at low temperatures. International Journal of Thermal Sciences, 2007, 46(3): 294–299.

[21] Du K., et al. A study on the cycle characteristics of an auto-cascade refrigeration system. Experimental Thermal and Fluid Science, 2009, 33(2): 240–245.

[22] Missimer D. J. Refrigerant conversion of auto-refrigerating cascade (ARC) systems. International Journal of Refrigeration, 1997, 20(3): 201–207.

[23] Wang Q., et al. An investigation of the mixing position in the recuperators on the performance of an auto-cascade refrigerator operating with a rectifying column. Cryogenics, 2012, 52(11): 581–589.

[24] Wang Q., et al. Numerical investigations on the performance of a single-stage auto-cascade refrigerator operating with two vapor–liquid separators and environmentally benign binary refrigerants. Applied Energy, 2013, 112: 949–955.

[25] Yan G., Hu H., and Yu J.. Performance evaluation on an internal auto-cascade refrigeration cycle with mixture refrigerant R290/R600a. Applied Thermal Engineering, 2015. 75: 994–1000.

[26] Tan Y., Wang L., and Liang K., Thermodynamic performance of an auto-cascade ejector refrigeration cycle with mixed refrigerant R32 + R236fa. Applied Thermal Engineering, 2015, 84: 268–275.

[27] Gong M.Q., Wu J.F., and Luo E.C.. Performances of the mixed-gases Joule–Thomson refrigeration cycles for cooling fixed-temperature heat loads. Cryogenics, 2004, 44(12): 847–857.

[28] Yan G., Chen J., and Yu J.. Energy and exergy analysis of a new ejector enhanced auto-cascade refrigeration cycle. Energy Conversion and Management, 2015, 105: 509–517.

[29] Keenan H., Neumann, E.P. and Lustwer K, F. An investigation of ejector design by analysis and experiment. Journal of Applied Mechanics-transactions of the ASME, 1950, ASME 72: 299–309.

[30] Wang J., Y. Dai, and Z. Sun. A theoretical study on a novel combined power and ejector refrigeration cycle. International Journal of Refrigeration, 2009, 32(6): 1186–1194.

[31] Yu J., Song X., and Ma M.. Theoretical study on a novel R32 refrigeration cycle with a two-stage suction ejector. International Journal of Refrigeration, 2013, 36(1): 166–172.

[32] NIST thermodynamic and transport properties of refrigerants and refrigerant mixtures REFPROP. 2002, NIST Standard Reference Database 23.

[33] Alexis G.K. and Katsanis J.S.. Performance characteristics of a methanol ejector refrigeration unit. Energy Conversion and Management, 2004, 45(17): 2729–2744.